THE ASTRONOMICAL JOURNAL, 117:1042–1055, 1999 February

STELLAR ENCOUNTERS WITH THE OORT CLOUD BASED ON *HIPPARCOS* DATA

JOAN GARCÍA-SÁNCHEZ,[1] ROBERT A. PRESTON, DAYTON L. JONES, AND PAUL R. WEISSMAN
Jet Propulsion Laboratory, California Institute of Technology, 4800 Oak Grove Drive, Pasadena, CA 91109
JEAN-FRANÇOIS LESTRADE
Observatoire de Paris-Section de Meudon, Place Jules Janssen, F-92195 Meudon, Principal Cedex, France
AND
DAVID W. LATHAM AND ROBERT P. STEFANIK
Harvard-Smithsonian Center for Astrophysics, 60 Garden Street, Cambridge, MA 02138
Received 1998 May 15; accepted 1998 September 4

ABSTRACT

We have combined *Hipparcos* proper-motion and parallax data for nearby stars with ground-based radial velocity measurements to find stars that may have passed (or will pass) close enough to the Sun to perturb the Oort cloud. Close stellar encounters could deflect large numbers of comets into the inner solar system, which would increase the impact hazard at Earth. We find that the rate of close approaches by star systems (single or multiple stars) within a distance D (in parsecs) from the Sun is given by $N = 3.5D^{2.12}$ Myr^{-1}, less than the number predicted by a simple stellar dynamics model. However, this value is clearly a lower limit because of observational incompleteness in the *Hipparcos* data set. One star, Gliese 710, is estimated to have a closest approach of less than 0.4 pc 1.4 Myr in the future, and several stars come within 1 pc during a ± 10 Myr interval. We have performed dynamical simulations that show that none of the passing stars perturb the Oort cloud sufficiently to create a substantial increase in the long-period comet flux at Earth's orbit.

Key words: comets: general — solar neighborhood — solar system: general — stars: kinematics

1. INTRODUCTION

The solar system is surrounded by a vast cloud of $\sim(10^{12}$–$10^{13})$ comets with orbits extending to interstellar distances, called the Oort cloud, and with a total estimated mass of some tens of Earth masses (Oort 1950; for a recent review see Weissman 1996a). The boundary of stable cometary orbits, which is the outer dimension of the Oort cloud, is a prolate spheroid with the long axis oriented toward the Galactic nucleus, and with maximum semimajor axes of about 10^5 AU for direct orbits of comets oriented along the Galactic radius vector, about 8×10^4 AU for orbits perpendicular to the radius vector, and about 1.2×10^5 AU for retrograde orbits (those opposite to the direction of Galactic rotation) (Smoluchowski & Torbett 1984; Antonov & Latyshev 1972). These cometary orbits are perturbed by random passing stars, by giant molecular clouds, and by the Galactic gravitational field. In particular, close or penetrating passages of stars through the Oort cloud can deflect large numbers of comets into the inner planetary region (Hills 1981; Weissman 1996b), initiating Earth-crossing cometary showers and possible collisions with Earth. Sufficiently large impacts or multiple impacts closely spaced in time could result in biological extinction events. Some terrestrial impact craters and stratigraphic records of impact and extinction events suggest that such showers may have occurred in the past (Farley et al. 1998). Dynamical models (e.g., Hut el al. 1987; Fernandez & Ip 1987) show that a cometary shower has a typical duration of about 2–3 Myr.

Evidence of the dynamical influence of close stellar passages on the Oort cloud might be found in the distribution of cometary aphelion directions. Although the distribution of long-period (10^6–10^7 yr) comet aphelia is largely isotropic on the sky, some nonrandom clusters of orbits exist, and it has been suggested that these groupings record the tracks of recent stellar passages close to the solar system (Biermann, Huebner, & Lüst 1983). However, Weissman (1993) showed that it would be difficult to detect a cometary shower in the orbital element distributions of the comets, except for the inverse semimajor axis ($1/a_0$) energy distribution, and that there is currently no evidence of a cometary shower in this distribution.

Some work has been done in the past to search for stellar perturbers of the cometary cloud. Mülläri & Orlov (1996) used ground-based telescopic data to predict close encounters with the Sun by stars contained in the Preliminary Version of the Third Catalogue of Nearby Stars (Gliese & Jahreiss 1991). They found that in the past, three stars may have had encounters with the Sun within 2 pc, and that in the future, 22 may have them. Matthews (1994) made a similar study, which was limited to stars in the solar neighborhood within a radius of about 5 pc, and he listed close approach distances for six stars in the near future, within the next 5×10^4 yr.

However, the accuracy of most ground-based parallax and proper-motion measurements is limited to several milliarcseconds or milliarcseconds per year, respectively. This measurement accuracy imposes a severe limitation on the accuracy of predictions of past or future close stellar passages.

Using parallax and proper-motion data from the *Hipparcos* satellite, we have selected a sample of nearby stars that might have passed or will pass close to the Sun, in order to identify those passages that might cause a significant perturbation on the orbits of comets in the Oort cloud. We have then used radial velocity measurements from the astronomical literature to reconstruct the three-dimensional trajectories of these stars. We also measured

[1] Also Departament d'Astronomia i Meteorologia, Universitat de Barcelona, Avenida Diagonal 647, E-08028 Barcelona, Spain.

radial velocities for some of the stars, most of them with no previous measurements. The *Hipparcos* mission provided very accurate parallax and proper-motion measurements for 118,218 stars, with a median precision of less than 1 mas and 1 mas yr^{-1}, respectively (ESA 1997). The *Hipparcos* proper motions are consistent with an inertial system within ± 0.25 mas yr^{-1}, as determined by the link between the *Hipparcos* Reference Frame and the International Celestial Reference System (ICRS).

In this paper we identify stars in our sample that could have a close passage by (1) assuming a simple rectilinear motion model; and (2) performing dynamical integrations of the motion of the stars in the Galactic potential. We also estimate the frequency of stellar encounters with the solar system. Close stellar passages mainly perturb comets near their aphelia, causing changes in the perihelion distance and inclination of the orbits of long-period comets. For those stellar passages that most likely could affect the cometary orbits, we have modeled the perturbations through dynamical simulations. In future papers we will report the individual radial velocities we have measured, with a discussion of the orbital solutions for nonsingle stars, and we will study the stellar passages using a larger sample and a range of Galactic potentials.

2. OBSERVATIONAL DATA AND ANALYSIS

Significant perturbations of the Oort cloud may be possible out to a distance of about 2–3 pc. We selected 1194 stars from the *Hipparcos* Catalogue (ESA 1997), whose proper motion, combined with an assumed maximum radial velocity of 100 km s^{-1}, implied an impact parameter of ≤ 3 pc. This radial velocity is 2–3 times the local stellar velocity dispersion, to allow intrinsically higher velocity stars to be included. At that velocity, this requirement meant that stars whose proper motion in milliarcseconds per year was less than 0.06 times the square of the parallax in milliarcseconds (for parallax values greater than 4.5 mas) are the best candidates to have approaches within 3 pc from the Sun over about ± 10 Myr from the present epoch. For smaller parallax values the implied proper-motion limit is close to or below the *Hipparcos* measurement accuracy.

In order to predict the past or future close stellar encounters with the Sun, we searched for published radial velocity measurements in the literature and also made new observations of several stars. We found values for 564 of our 1194 stars (about 47% of the sample), which were combined with the *Hipparcos* Catalogue data to calculate the time and distance of the close passages. The catalogue also provides the standard errors and the correlation coefficients of the astrometric data.

The selection criteria are based on a simple rectilinear motion model, and we have investigated several effects that might make this model inadequate. These effects include multiple scattering by other stars along a star's path toward or away from the Sun and differential acceleration between the Sun and the star due to the large-scale Galactic potential.

The effect of stellar interactions is small: a star passing 1 pc from a 1 $M_\odot$ star with a relative velocity of 20 km s^{-1} results in an angular deflection of only 4″.5. Even over a path length of 100 pc, the rms deflection due to such encounters (assuming a local stellar density of 0.1 pc^{-3}) is less than 1′. This deflection at 100 pc initial distance would change the impact parameter by less than 0.03 pc.

We also estimated the differential acceleration of the Sun and the nearby star in the Galactic potential. Assuming an axially symmetric and stationary Galactic potential field, the force laws parallel and perpendicular to the Galactic plane can be used to estimate this differential acceleration in the solar neighborhood. Using IAU Galactic parameters (Kerr & Lynden-Bell 1986), the change in the Sun-star encounter distance induced by the potential field from that given by a rectilinear motion, at a time equal to the time of closest approach T, can be estimated as

$$\delta_R \simeq 1.4 \times 10^{-4}\ \mathrm{pc} \left(\frac{T}{\mathrm{Myr}}\right)^2 \left(\frac{2d_R + d_{Rc}}{\mathrm{pc}}\right) \tag{1}$$

and

$$\delta_Z \simeq 7.1 \times 10^{-4}\ \mathrm{pc} \left(\frac{T}{\mathrm{Myr}}\right)^2 \left(\frac{2d_Z + d_{Zc}}{\mathrm{pc}}\right) \tag{2}$$

in the Galactic plane and perpendicular directions, respectively, where d_R is the difference between the current galactocentric distance of the Sun and that of the star in the Galactic midplane, d_{Rc} is the difference at time T, d_Z is the difference between the current vertical distance of the Sun and the star from the midplane, and d_{Zc} the difference at time T. The change in encounter distance for time T may be estimated as $\delta_{\mathrm{total}} = (\delta_R^2 + \delta_Z^2)^{1/2}$.

This change is small for most of the stars in our sample, although it could be important for a few stars. Note that δ_{total} is proportional to T^2, so the largest deviations from rectilinear motion are expected for stars with large encounter times.

We also consider the Galactic orbital motion of the stars under the influence of the Galactic potential. Assuming an axisymmetric and steady-state (time-independent) potential, ψ, the equations of motion in cylindrical coordinates (R, θ, z) are given by

$$\frac{d^2R}{dt^2} - R\left(\frac{d\theta}{dt}\right)^2 = -\frac{\partial\psi}{\partial R}\,, \tag{3}$$

$$R^2\,\frac{d^2\theta}{dt^2} + 2\,\frac{dR}{dt}\,\frac{d\theta}{dt} = 0\,, \tag{4}$$

$$\frac{d^2z}{dt^2} = -\frac{\partial\psi}{\partial z}\,. \tag{5}$$

We assume that for small z/R the star's motion in the z direction can be decoupled from its motion in the Galactic plane. For the distances involved in our study this is a good approximation. The potential profile does not change much along the star's trajectory for the stars considered in the sample. Expanding the Galactic force field in the plane to first order around the Sun's galactocentric distance $R_\odot$, the following empirical expression for the radial force K_R can be derived:

$$K_R \simeq K_{R\odot} + \left(\frac{dK_R}{dR}\right)_\odot (R - R_\odot)\,. \tag{6}$$

Using $K_R = -\partial\psi/\partial R$ and introducing the Oort constants A and B, we obtain

$$\frac{\partial\psi}{\partial R} \simeq \left(\frac{\partial\psi}{\partial R}\right)_\odot + \frac{d}{dR}\left(\frac{\partial\psi}{\partial R}\right)_\odot (R - R_\odot) = (A - B)^2 R_\odot - (A - B)(3A + B)(R - R_\odot)\,, \tag{7}$$

TABLE 1

CfA Radial Velocities

HIP[a]	T_{eff} [b]	$v \sin i$ [c]	Nobs[d]	Time Span[e]	V[f]	Error[g]	Ext[h]	Int[i]	e/i[j]	χ^2	$P(\chi^2)$[k]	Comments[l]
1463	3750	0	4	392	−15.15	0.36	0.42	0.72	0.59	0.79	0.851769	
11048	3750	0	2	1131	−37.49	0.31	0.40	0.44	0.91	0.84	0.360620	U039
11559	7250	10	4	408	20.87	0.83	1.67	0.73	2.29	16.43	0.000925	S?
20359	4500	0	4	343	−78.51	0.18	0.31	0.36	0.86	2.78	0.426808	U077
20917	4500	0	60	4323	−35.19	0.06	0.44	0.41	1.06	67.10	0.219143	Gl 169
21158	6250	0	5	1462	6.78	0.16	0.31	0.35	0.89	3.08	0.543902	H028676
21386	6500	10	7	1010	−50.72	1.37	3.63	0.68	5.33	204.55	0.000000	H026367, S
23452	3750	0	1	0	−17.13	0.43	0.00	0.43	0.00	0.00	1.000000	U092, CCDM
23913	5500	0	4	383	−26.97	0.26	0.53	0.49	1.08	5.54	0.136311	
26335	3750	0	4	378	21.90	0.23	0.09	0.46	0.20	0.16	0.983637	U105
30067	6250	0	6	1552	40.19	0.14	0.24	0.35	0.68	2.39	0.792919	H043947
30920	3500	0	69	4364	17.93	0.15	1.27	1.08	1.18	106.92	0.001814	Gl 234, CCDM
31626	4500	0	2	76	82.68	0.24	0.08	0.34	0.23	0.05	0.814880	U117
33275	6500	10	3	320	−14.45	0.25	0.34	0.43	0.78	1.13	0.567759	
35136	6000	0	6	1758	84.20	0.20	0.32	0.50	0.65	2.51	0.774867	H055575
36208	3750	0	66	5258	18.23	0.12	0.60	0.97	0.61	23.59	0.999999	Gl 273
38228	5750	10	6	1587	−15.93	0.22	0.19	0.54	0.35	1.01	0.961815	H063433
39986	8750	120	6	455	26.39	7.43	18.20	5.73	3.18	40.81	0.000000	S
40317	5750	0	3	329	34.18	0.24	0.28	0.42	0.67	1.03	0.596886	
41820	5500	0	8	1870	−16.12	0.18	0.51	0.34	1.52	17.38	0.015121	CCDM
49908	4500	0	134	4444	−25.92	0.04	0.44	0.33	1.33	226.52	0.000001	Gl 380, CCDM
52097	6500	30	7	340	−9.25	0.58	0.88	1.52	0.58	1.71	0.944082	CCDM
57548	3750	0	16	4033	−30.85	0.27	0.81	1.07	0.76	8.47	0.903657	U223
75311[m]	6000	0	4	355	−13.87	0.31	0.22	0.62	0.35	0.33	0.953365	CCDM
75311[n]	6250	0	4	355	−14.80	0.27	0.26	0.53	0.49	0.80	0.849277	CCDM
79667	9250	70	3	329	−18.86	2.11	1.25	3.66	0.34	0.49	0.782547	
80459	3750	0	5	3802	−13.03	0.28	0.43	0.63	0.68	1.82	0.769203	U342
80824	3750	0	19	1006	−21.04	0.23	0.93	1.00	0.93	12.90	0.797476	U347, CCDM
81935	4750	0	2	85	−19.07	0.18	0.25	0.25	1.03	1.07	0.300651	
82003	4500	0	139	4446	−31.35	0.04	0.50	0.34	1.45	308.57	0.000000	Gl 638
85605	5000	0	4	232	−21.11	0.24	0.49	0.42	1.15	4.15	0.245367	CCDM
85661	7500	90	6	385	−45.98	1.67	4.10	2.39	1.71	15.83	0.007344	CCDM
86961	4500	0	1	0	−28.87	0.88	0.00	0.88	0.00	0.00	1.000000	CCDM
86963	3750	20	1	0	−27.36	2.28	0.00	2.28	0.00	0.00	1.000000	CCDM
88574	3750	0	1	0	32.06	0.60	0.00	0.60	0.00	0.00	1.000000	U387
89825	4250	0	5	526	−13.90	0.19	0.16	0.41	0.39	0.59	0.963754	
90112	5250	0	2	58	25.95	0.28	0.13	0.39	0.32	0.10	0.746999	
91768	3750	0	62	4933	−0.93	0.10	0.51	0.76	0.67	26.88	0.999956	Gl 725A, CCDM
91772	3750	0	59	4933	1.22	0.11	0.57	0.83	0.68	29.32	0.999390	Gl 725B, CCDM
92403	3500	0	1	0	−11.48	0.82	0.00	0.82	0.00	0.00	1.000000	U401
94512	8750	60	4	186	−30.67	1.75	3.50	2.04	1.72	6.22	0.101272	
94761	3750	0	4	783	35.38	0.39	0.44	0.77	0.57	0.99	0.804676	U412
95326	5000	10	2	58	35.56	0.42	0.11	0.59	0.19	0.04	0.846828	CCDM
99483	4750	0	3	169	25.03	0.23	0.23	0.40	0.58	0.72	0.696622	
100111	5750	0	4	120	26.07	0.28	0.57	0.52	1.10	2.94	0.401470	
101573	4750	0	3	481	43.65	0.51	0.88	0.53	1.65	5.94	0.051326	
103039	3750	0	3	155	15.82	0.56	0.59	0.97	0.61	0.77	0.681886	
103659	6750	20	3	66	−15.79	0.58	0.46	1.01	0.45	0.41	0.814551	
107528	6750	19	4	293	−7.23	0.36	0.72	0.68	1.07	2.87	0.411325	
110893	3750	0	31	2164	−33.77	0.16	0.78	0.87	0.90	17.66	0.963768	U483, CCDM
113020	3750	0	87	3746	−1.81	0.11	0.82	1.00	0.82	58.10	0.990909	Gl 876
117473	3750	0	48	4431	−71.16	0.09	0.46	0.62	0.75	27.74	0.988624	Gl 908
117748	7500	30	4	269	7.38	0.66	0.76	1.33	0.57	0.82	0.845559	CCDM

[a] *Hipparcos* Catalogue number.

[b] Effective temperature adopted for the synthetic template spectrum (in K).

[c] Rotational velocity (in km s^{-1}).

[d] Number of observations.

[e] Time span between the first and last observations (in days).

[f] Average velocity (in km s^{-1}).

[g] Standard deviation of the average velocity (in km s^{-1}).

[h] External rms deviation of the individual velocities from the mean (in km s^{-1}).

[i] Average of the internal velocity error estimates from our cross-correlation package, XCSAO (Kurtz et al. 1992) running under the IRAF environment. IRAF (Image Reduction and Analysis Facility) is distributed by the National Optical Astronomy Observatories, which are operated by the Association of Universities for Research in Astronomy, Inc., under contract with the National Science Foundation.

[j] Ratio of the external to internal errors.

[k] Probability that a constant velocity star might accidentally show a χ^2 value larger than we actually observe.

[l] Name assigned by the CfA observing catalogs if the star was originally observed for another project. In a few cases a code for suspected single-lined binaries, S?, and definite velocity variables, S, is given. CCDM indicates stars listed in the Catalogue of Components of Double and Multiple Stars (Dommanget & Nys 1994).

[m] Northwest component.

[n] Southeast component.

where

$$A = \frac{1}{2}\left[\frac{\Theta_\odot}{R_\odot} - \left(\frac{d\Theta}{dR}\right)_\odot\right] = -\frac{1}{2} R_\odot \left(\frac{d\omega}{dR}\right)_\odot , \tag{8}$$

$$B = -\frac{1}{2}\left[\frac{\Theta_\odot}{R_\odot} + \left(\frac{d\Theta}{dR}\right)_\odot\right] , \tag{9}$$

$$\left(\frac{d\Theta}{dR}\right)_\odot = -(A + B) , \tag{10}$$

$$\omega_\odot = A - B , \tag{11}$$

with $\Theta_\odot$ and $\omega_\odot$ being the circular and angular velocity of Galactic rotation, respectively, at the Sun.

For the perpendicular motion about the Galactic plane we can use the third equation of motion (eq. [5]), where the right-hand term is related to the vertical force K_z through $K_z = -\partial\psi/\partial z$, and K_z is related to the total mass density in the neighborhood of the Sun, $\rho_\odot$, through Poisson's equation, which, to first order, is

$$4\pi G\rho_\odot = -\frac{\partial K_z}{\partial z} , \tag{12}$$

The term neglected in this equation, $2(A^2 - B^2)$, is zero for a flat Galactic rotation curve and is small for other rotation curves.

2.1. *Radial Velocities*

Radial velocity measurements were obtained from the astronomical literature, in particular the compilations of Wilson (1953), Evans (1978), and others, but also from other miscellaneous sources. For some stars the radial velocity uncertainty is not reported in the literature, and in these cases we assume an uncertainty of 3 km s^{-1}.

We also measured new radial velocities for some of the stars in our sample. For these observations we used the Center for Astrophysics (CfA) digital speedometers (Latham 1985, 1992), primarily on the 1.5 m Wyeth Reflector at the Oak Ridge Observatory in Harvard, Massachusetts, but also on the 1.5 m Tillinghast Reflector and the Multiple Mirror Telescope at the F. L. Whipple Observatory atop Mount Hopkins, Arizona.

The radial velocities were derived using cross-correlation techniques following the general approach outlined in Nordström et al. (1994). The templates were drawn from an extensive grid of synthetic spectra calculated by J. Morse using Kurucz (1992a, 1992b) model atmospheres. For the template parameters we adopted solar metallicity and surface gravity log $g = 4.5$ throughout and ran extensive grids of correlations in effective temperature and rotational velocity in order to determine the template that gave the highest peak correlation value averaged over all the exposures. These techniques yield a precision of about 0.5 km s^{-1} for a single-velocity measurement of a slowly rotating solar-type star, with an absolute accuracy of about 0.1 km s^{-1} in the zero point of the CfA velocity system. The precision of a single-velocity measurement degrades with increasing rotational velocity and can be as poor as 2 or 3 km s^{-1} near the limiting value of v sin i, about 140 km s^{-1}, that can be handled by the CfA procedures. For the coolest M dwarfs and for stars with very rapid rotation, the absolute zero point of the CfA velocity system may be uncertain by as much as 1 km s^{-1} because of template mismatch. The results of the CfA velocity measurements for the stars included in this paper are summarized in Table 1.

It is important to identify spectroscopic binaries among our targets, because orbital motion can introduce a significant deviation of a single-velocity measurement from the center-of-mass velocity for the system, especially for short-period binaries where the orbital amplitude can be tens of km s^{-1}. We include indicators of possible binary systems in Table 1. The ratio of the external to internal errors, e/i (see Table 1 for details), is often used as an indicator of intrinsic velocity variation. Stars with $e/i > 2$ may be identified as binaries. However, for stars with just a few observations we prefer to use $P(\chi^2)$, the probability that a constant velocity star might show, by accident, a χ^2 value larger than we actually observe. Stars with $P(\chi^2)$ less than or equal to about 0.001 are very unlikely to be intrinsically constant.

The e/i test is not well suited for stars with only a few observations, because the external error estimate is vulnerable to statistical fluctuations. $P(\chi^2)$ is a less useful test for stars with many observations because it assumes that the errors are exactly Gaussian, while real data sets always have outliers. Very subtle deficiencies in the internal error estimates can get translated into extreme values of $P(\chi^2)$ for stars with dozens of observations. This problem is illustrated by the results for the M dwarfs with Gliese identifications in Table 1. Those targets have been observed for many years for another project and have much richer data sets than the stars that were new targets for the present project.

Two of the stars in Table 1, HIP 21386 and 39986, have large e/i ratios and very small $P(\chi^2)$ values. Plots of the velocity histories for these stars confirm that there are significant variations in their velocities, and there is little doubt that they are binaries. The error indicators for one of the stars, HIP 11559, suggest that it may also be a variable, but the evidence is very marginal.

The stars in Table 1 include two visual binaries: HIP 75311, which has an angular separation of 3".25, and HIP 91768 and 91772 (Gl 725A and 725B), which are separated by 13".3. For each of these systems the velocities of the individual members are quite similar, confirming the conclusion already reported in the *Hipparcos* data base that they are physical binaries. In both cases the member stars must have nearly the same masses because they have very similar brightnesses, so it should be adequate to calculate the center-of-mass velocity simply by averaging the velocities of the two components. For HIP 75311 this gives a system velocity of -14.3 ± 0.3 km s^{-1}, and for Gl 725, a system velocity of 0.15 ± 0.1 km s^{-1}.

3. RESULTS

For the calculation of the stellar passages we have used both a straight-line–motion approximation and integrated orbits using the equations of motion for the Galactic potential given above. For the integrated orbits we have used a fourth-order Runge-Kutta integrator. Oort constants $A = 14.82 \pm 0.84$ km s^{-1} kpc^{-1} and $B = -12.37 \pm 0.64$ km s^{-1} kpc^{-1}, and $R_\odot = 8.5 \pm 0.5$ kpc, are adopted from Feast & Whitelock (1997) and the local total mass density $\rho_\odot = 0.076 \pm 0.015\ M_\odot$ pc^{-1} from Crézé et al. (1998).

The stars we find with a closest approach distance within 5 pc of the Sun are listed in Table 2 in order of increasing miss distance. These predicted passages are contained in a time interval of about ± 10 Myr, with most occurring

TABLE 2

STELLAR PASSAGES WITHIN 5 PC OF THE SUN

HIP[a]	Name[b]	R.A.[c]	Decl.[c]	T_{int} [d]	T_{lin} [d]	σ_T [e]	D_{int} [f]	D_{lin} [f]	σ_D [g]	V_r [h]	Reference[i]
89825	Gl 710	18 19 50.84	−01 56 19.0	1357.8	1357.3	41.8	0.336	0.343	0.161	−13.9	CfA
85661	HD 158576	17 30 20.00	−04 22 09.8	1846.5	1845.8	150.4	0.846	0.753	0.677	−46.0	CfA
70890	Proxima	14 29 47.75	−62 40 52.9	26.7	26.7	0.2	0.954	0.954	0.036	−21.7	1
71683	α Centauri A	14 39 40.90	−60 50 06.5	27.8	27.8	0.1	0.973	0.973	0.021	−22.7	2
71681	α Centauri B	14 39 39.39	−60 50 22.1	27.7	27.7	0.2	0.975	0.975	0.021	−22.7	2
57544	AC +79°3888	11 47 39.17	+78 41 24.0	42.8	42.8	0.9	1.007	1.007	0.025	−119.0	3
80300	Gl 620.1B	16 23 33.78	−39 13 46.2	−241.9	−241.8	11.8	1.139	1.139	0.095	51.4	4
87937	Barnard's star	17 57 48.97	+04 40 05.8	9.7	9.7	0.0	1.143	1.143	0.006	−110.9	5
100111	HD 351880	20 18 30.60	+19 01 51.8	−944.7	−944.8	775.3	1.439	1.445	3.630	26.1	CfA
54035	Lalande 21185	11 03 20.61	+35 58 53.3	20.0	20.0	0.0	1.440	1.440	0.006	−84.7	5
11559	SAO 75395	02 28 54.92	+21 11 22.7	−5477.0	−5541.7	1069.0	1.448	2.688	4.007	20.9	CfA
94512	HD 179939	19 14 10.04	+07 45 50.7	3734.0	3732.9	451.0	1.451	1.025	1.142	−30.7	CfA
26335	Gl 208	05 36 30.99	+11 19 40.8	−497.9	−497.9	8.6	1.600	1.599	0.058	21.9	CfA
26624	HD 37594	05 39 31.15	−03 33 53.0	−1804.2	−1804.1	117.7	1.610	1.598	0.258	22.4	6
27288	Gl 217.1	05 46 57.35	−14 49 19.0	−1045.9	−1046.0	130.1	1.637	1.629	0.217	20.0	3
99483	HIP 99483	20 11 24.07	+05 36 19.9	−2892.5	−2894.9	1452.0	1.653	1.379	25.299	25.0	CfA
25240	HD 35317	05 23 51.33	−00 51 59.8	−1078.0	−1077.9	77.7	1.755	1.735	0.531	52.6	7
86963	GJ 2130B	17 46 14.47	−32 06 06.0	202.6	202.6	18.6	1.782	1.782	0.264	−27.4	CfA
103738	HD 19995	21 01 17.46	−32 15 28.0	−3781.5	−3802.2	230.7	1.811	2.653	1.111	17.6	3
101573	HIP 101573	20 35 07.18	+07 43 07.1	−4189.0	−4202.4	1805.7	1.821	1.898	6.108	43.6	CfA
85605	CCDM 17296+2439B	17 29 36.19	+24 39 11.6	196.8	196.8	28.3	1.837	1.837	0.695	−21.1	CfA
47425	Gl 358	09 39 46.78	−41 04 06.3	−62.8	−62.8	8.6	1.875	1.875	0.273	142.0	8
92403	Ross 154	18 49 48.96	−23 50 08.8	151.8	151.8	2.2	1.881	1.881	0.082	−11.5	CfA
40317	HD 68814	08 13 57.11	−04 03 12.6	−2346.0	−2347.3	298.8	1.909	1.990	1.341	34.2	CfA
57548	Ross 128	11 47 44.04	+00 48 27.1	71.1	71.1	0.3	1.911	1.911	0.027	−30.9	CfA
86961	GJ 2130A	17 46 12.66	−32 06 10.0	189.0	189.0	13.2	1.929	1.929	0.366	−28.9	CfA
110893	Gl 860A	22 28 00.42	+57 41 49.3	88.6	88.6	0.6	1.949	1.949	0.043	−33.8	CfA
23641	HD 33487	05 04 53.49	−69 10 08.0	1040.7	1041.5	139.1	1.977	1.954	0.372	−39.0	9
30067	HD 43947	06 19 40.18	+16 00 47.8	−666.4	−666.3	16.5	2.016	2.016	0.117	40.2	CfA
21386	HD 26367	04 35 24.09	+85 31 37.2	704.4	704.5	42.5	2.028	2.038	0.285	−50.7	CfA
35550	Gl 271A	07 20 07.39	+21 58 56.4	1138.0	1138.0	111.7	2.038	2.029	1.169	−15.3	10
20359	Gl 168	04 21 35.92	+48 20 13.1	380.5	380.5	22.5	2.074	2.075	0.288	−78.5	CfA
16537	Gl 144	03 32 56.42	−09 27 29.9	−104.8	−104.9	0.8	2.135	2.135	0.079	16.8	7
38228	HD 63433	07 49 55.07	+27 21 47.6	1326.2	1326.4	31.4	2.138	2.121	0.123	−15.9	CfA
86214	Gl 682	17 37 04.24	−44 19 01.0	67.4	67.4	15.1	2.140	2.140	0.616	−60.0	8
13772	Gl 120.1	02 57 14.69	−24 58 09.9	−429.9	−430.0	34.8	2.245	2.246	0.276	50.6	11
86990	Gl 693	17 46 35.44	−57 18 56.7	42.0	42.0	0.9	2.253	2.253	0.073	−115.0	11
95326	CCDM 19236−3911B	19 23 38.93	−39 11 21.0	−342.9	−342.9	239.3	2.261	2.260	3.754	35.6	CfA
68634	HD 122676	14 02 56.90	+14 58 31.2	−305.4	−305.4	50.9	2.263	2.262	0.392	83.0	12
77257	Gl 598	15 46 26.75	+07 21 11.7	165.7	165.7	1.6	2.267	2.267	0.044	−66.8	13
13769	Gl 120.1C	02 57 13.18	−24 58 30.1	−503.1	−503.2	35.6	2.269	2.269	0.217	49.6	11
8709	WD 0148+467	01 52 02.96	+47 00 05.6	−237.2	−237.2	13.7	2.286	2.286	0.270	64.0	11
32349	Sirius	06 45 09.25	−16 42 47.3	65.7	65.7	5.5	2.299	2.299	0.089	−9.4	14
26744	HD 37574	05 40 57.82	+32 53 45.6	6122.0	6054.1	1546.9	2.305	2.233	1.233	−10.0	3
113421	HD 217107	22 58 15.54	−02 23 43.2	1405.8	1408.5	173.6	2.313	2.323	0.311	−13.5	7
93506	HD 176687	19 02 36.72	−29 52 48.4	−1205.6	−1205.2	142.2	2.314	2.333	0.434	22.0	3
75311	BD −02°3986	15 23 11.60	−02 46 00.5	3961.0	3987.4	1637.9	2.316	3.102	8.542	−14.3	CfA
39986	HD 67852	08 09 58.46	+01 01 13.8	−4378.0	−4384.4	1357.2	2.341	1.229	2.951	26.4	CfA
31626	HD 260564	06 37 05.29	+19 45 10.7	−405.2	−405.2	28.4	2.341	2.340	0.339	82.7	CfA
14576	Algol	03 08 10.13	+40 57 20.3	−6916.0	−6895.4	867.6	2.381	2.666	0.632	4.0	3
5643	Gl 54.1	01 12 29.90	−17 00 01.9	−74.4	−74.4	1.1	2.429	2.429	0.162	28.0	3
103039	LP 816−60	20 52 33.20	−16 58 29.3	−269.9	−269.9	6.4	2.482	2.483	0.123	15.8	CfA
33275	HD 50867	06 55 17.44	+05 54 37.7	3480.5	3472.8	182.9	2.587	2.732	0.937	−14.4	CfA
1463	Gl 16	00 18 16.59	+10 12 10.3	1018.4	1019.2	41.2	2.609	2.623	0.236	−15.2	CfA
25001	HD 34790	05 21 12.69	+29 34 11.6	4484.0	4456.5	350.0	2.647	2.862	1.948	−18.7	3
85429	IRAS 17249+0416	17 27 25.94	+04 13 39.1	542.5	542.5	327.9	2.664	2.658	1.924	−90.0	16
82977	HD 152912	16 57 22.64	−25 47 58.5	−2727.5	−2722.8	734.6	2.700	2.466	3.821	50.0	3
97649	Gl 768	19 50 46.68	+08 52 02.6	139.5	139.5	1.2	2.702	2.702	0.043	−26.1	17
72511	CD−25 10553	14 49 33.51	−26 06 21.7	−72.9	−72.9	2.0	2.758	2.758	0.442	33.0	8
116727	Gl 903	23 39 20.98	+77 37 55.1	300.1	300.1	4.9	2.791	2.792	0.059	−43.1	7
91726	HD 172748	18 42 16.42	−09 03 09.2	1248.8	1248.5	66.0	2.806	2.823	0.374	−44.8	17
6379	Gl 56.5	01 21 59.20	+76 42 37.3	704.0	704.0	35.7	2.823	2.823	0.157	−22.7	3
117473	Gl 908	23 49 11.95	+02 24 12.9	62.8	62.9	0.3	2.886	2.885	0.046	−71.2	CfA
116250	HD 221420	23 33 19.55	−77 23 07.2	−1183.3	−1184.4	18.2	2.907	2.886	0.127	26.0	15
77910	HD 142500	15 54 40.27	+08 34 49.2	2860.0	2873.9	361.9	2.917	2.458	1.070	−25.1	17
30920	Ross 614	06 29 23.00	−02 48 44.9	−110.9	−110.9	0.2	2.929	2.929	0.050	17.9	CfA

TABLE 2—*Continued*

HIP[a]	Name[b]	R.A.[c]	Decl.[c]	T_{int} [d]	T_{lin} [d]	σ_T [e]	D_{int} [f]	D_{lin} [f]	σ_D [g]	V_r [h]	Reference[i]
35136	GJ 1095	07 15 50.11	+47 14 25.5	−189.7	−189.7	2.1	2.969	2.968	0.068	84.2	CfA
37766	Ross 882	07 44 40.38	+03 33 12.8	−160.3	−160.3	1.4	3.052	3.052	0.084	26.6	5
72509	Gl 563.2B	14 49 32.69	−26 06 40.2	−71.6	−71.6	4.1	3.071	3.070	1.480	33.0	8
80543	HD 148317	16 26 39.21	+15 58 21.5	2103.0	2108.0	198.0	3.132	2.903	0.640	−37.0	3
81935	HD 150689	16 44 15.03	−38 56 36.6	701.7	701.6	10.9	3.145	3.146	0.093	−19.1	CfA
20917	Gl 169	04 29 00.17	+21 55 20.2	294.1	294.1	3.0	3.189	3.188	0.077	−35.2	CfA
36795	Gl 279	07 34 03.21	−22 17 46.3	−411.7	−411.7	7.1	3.196	3.197	0.107	60.1	18
80824	Gl 628	16 30 18.11	−12 39 35.0	86.0	86.0	0.2	3.208	3.208	0.039	−21.0	CfA
86162	Gl 687	17 36 26.41	+68 20 32.0	78.8	78.8	0.2	3.213	3.213	0.378	−27.9	19
29271	Gl 231	06 10 14.20	−74 45 09.1	−255.2	−255.2	3.1	3.249	3.249	0.050	34.9	17
27075	HD 38382	05 44 28.41	−20 07 36.0	−634.7	−634.8	45.9	3.271	3.273	0.266	38.7	7
8102	Gl 71	01 44 05.13	−15 56 22.4	42.6	42.6	0.5	3.271	3.271	0.016	−16.4	20
1242	Gl 1005	00 15 27.67	−16 07 56.3	105.8	105.8	3.4	3.289	3.289	0.509	−29.0	11
3829	Van Maanen's star	00 49 09.18	+05 23 42.7	−34.3	−34.3	0.3	3.327	3.327	0.137	54.0	21
21158	HD 28676	04 32 07.91	+21 37 56.5	−5628.0	−5612.1	241.0	3.380	2.966	1.236	6.8	CfA
91438	Gl 722	18 38 53.45	−21 03 05.4	−306.6	−306.6	17.4	3.384	3.384	0.217	38.6	7
23913	HD 233081	05 08 16.22	+52 22 03.3	1842.8	1841.8	131.4	3.396	3.355	0.750	−27.0	CfA
37279	Gl 280A	07 39 18.54	+05 13 39.0	29.6	29.6	7.1	3.438	3.438	0.032	−3.9	14
1475	Gl 15A	00 18 20.54	+44 01 19.0	−16.1	−16.1	0.2	3.469	3.469	0.014	11.9	5
85667	Gl 678	17 30 23.87	−01 03 45.0	200.9	201.0	4.4	3.503	3.503	0.160	−76.4	22
91772	Gl 725B	18 42 48.51	+59 37 20.5	−0.4	−0.4	0.2	3.515	3.515	0.062	0.1	CfA
103659......	HD 199881	21 00 08.69	−10 37 41.7	4926.0	4974.5	446.7	3.527	3.106	1.635	−15.8	CfA
39757	HD 67523	08 07 32.70	−24 18 16.0	−394.0	−394.0	6.1	3.563	3.564	0.096	46.1	23
91768	Gl 725A	18 42 48.22	+59 37 33.7	−0.4	−0.4	0.2	3.568	3.568	0.033	0.1	CfA
7751	Gl 66	01 39 47.24	−56 11 47.2	−283.5	−283.5	4.4	3.570	3.570	0.098	22.7	3
90112	HD 168769	18 23 19.64	−39 31 12.0	−1888.2	−1886.3	159.6	3.594	3.662	1.095	25.9	CfA
36208	Luyten's star	07 27 24.16	+05 14 05.2	−13.9	−13.9	0.1	3.666	3.666	0.021	18.2	CfA
105090......	Gl 825	21 17 17.71	−38 51 52.5	−19.6	−19.6	0.6	3.696	3.696	0.025	24.2	24
99701	Gl 784	20 13 52.75	−45 09 49.1	124.7	124.7	0.6	3.727	3.727	0.056	−31.1	17
98698	Gl 775	20 02 47.10	+03 19 33.2	372.5	372.5	20.1	3.756	3.756	0.242	−31.6	25
11048	Gl 96	02 22 14.46	+47 52 47.7	279.9	279.9	4.0	3.756	3.756	0.110	−37.5	CfA
33226	Gl 251	06 54 49.47	+33 16 08.9	−123.9	−123.9	0.3	3.814	3.814	0.063	22.7	5
117748......	BD +37°4901C	23 52 48.30	+38 41 10.8	−4387.0	−4426.2	1616.8	3.820	3.622	6.767	7.4	CfA
49908	Gl 380	10 11 23.36	+49 27 19.7	68.7	68.7	0.1	3.856	3.856	0.021	−25.9	CfA
33277	Gl 252	06 55 18.69	+25 22 32.3	1028.7	1028.6	61.0	3.867	3.862	0.275	−15.6	26
68184	HD 122064	13 57 32.10	+61 29 32.4	333.2	333.3	11.3	3.868	3.868	0.162	−25.3	3
57791	HD 102928	11 51 02.23	−05 20 00.0	−5593.0	−5789.0	493.1	3.939	2.744	1.169	13.4	27
89959	HD 168956	18 21 15.85	+26 42 24.3	2835.0	2840.6	345.7	3.940	3.762	1.085	−25.3	17
33909	HD 53253	07 02 15.48	−43 24 13.9	−3913.0	−3930.2	321.8	3.998	4.381	1.156	31.1	6
79667	HD 146214	16 15 33.26	−12 40 48.1	4840.0	4845.5	719.2	4.034	4.007	2.004	−18.9	CfA
101027......	Gl 791.1A	20 28 51.62	−17 48 49.2	−1578.8	−1578.8	106.6	4.053	4.103	0.416	18.4	3
34603	Gl 268	07 10 02.16	+38 31 54.4	−97.0	−97.0	0.5	4.066	4.066	0.143	37.9	28
99859	HD 192869	20 15 36.34	+42 21 43.4	3890.5	3905.4	471.4	4.080	4.072	1.689	−28.0	3
24502	HD 33959C	05 15 23.61	+32 41 05.1	1829.0	1827.0	1039.7	4.093	4.097	6.508	−13.1	29
45333	Gl 337.1	09 14 20.55	+61 25 24.2	1286.2	1287.2	44.6	4.121	4.121	0.181	−14.2	30
85523	Gl 674	17 28 39.46	−46 53 35.0	73.7	73.7	21.5	4.134	4.134	0.311	−10.2	31
80337	Gl 620.1A	16 24 01.24	−39 11 34.8	−867.5	−867.1	9.0	4.155	4.158	0.110	13.0	30
11964	Gl 103	02 34 22.52	−43 47 44.3	−233.2	−233.2	2.7	4.180	4.180	0.088	41.9	32
109555......	Gl 851	22 11 29.89	+18 25 32.7	188.2	188.2	2.7	4.203	4.203	0.148	−51.4	5
90595	HD 170296	18 29 11.85	−14 33 56.9	2129.0	2126.4	216.6	4.278	4.280	1.370	−41.0	3
27913	Gl 222	05 54 23.08	+20 16 35.1	471.7	471.6	2.6	4.380	4.380	0.080	−13.4	13
94761	Gl 752A	19 16 55.60	+05 10 19.7	−70.4	−70.4	0.1	4.420	4.420	0.055	35.4	CfA
114059......	HD 218200	23 05 56.62	+18 05 14.1	−4009.0	−4057.1	688.0	4.429	4.062	2.066	18.0	33
107528......	HD 207164	21 46 43.36	+19 28 37.5	9774.0	10153.1	845.2	4.449	7.785	3.524	−7.2	CfA
86400	Gl 688	17 39 17.02	+03 33 19.7	−381.4	−381.4	9.4	4.461	4.460	0.169	22.7	7
36186	HD 58954	07 27 07.99	−17 51 53.5	2870.0	2872.0	262.2	4.483	4.343	0.997	−29.2	3
90790	Gl 716	18 31 19.05	−18 54 30.0	274.7	274.7	4.3	4.484	4.484	0.121	−41.6	31
23452	HD 32450	05 02 28.51	−21 15 22.0	351.2	351.2	4.8	4.489	4.490	0.142	−17.1	CfA
87345	HD 162102	17 50 52.34	−33 42 20.4	3610.5	3595.6	603.4	4.518	4.629	2.972	−17.5	3
7981	Gl 68	01 42 29.95	+20 16 12.5	134.6	134.6	1.0	4.573	4.573	0.090	−33.9	26
41820	HD 71974	08 31 35.03	+34 57 58.3	1695.2	1697.5	67.2	4.612	4.564	0.486	−16.1	CfA
87777	HD 163547	17 55 50.81	+22 27 51.2	3351.0	3358.3	329.6	4.648	5.170	1.515	−43.6	3
113020......	Ross 780	22 53 16.16	−14 15 43.4	12.1	12.1	0.7	4.690	4.690	0.047	−1.8	CfA
88601	Gl 702	18 05 27.21	+02 30 08.8	75.2	75.2	8.2	4.698	4.698	0.113	−9.7	7
22449	Gl 178	04 49 50.14	+06 57 40.5	−211.3	−211.3	4.1	4.701	4.701	0.199	24.4	7
88574	Gl 701	18 05 07.25	−03 01 49.8	−150.6	−150.6	0.9	4.720	4.720	0.103	32.1	CfA
16536	Gl 145	03 32 56.11	−44 42 08.2	239.1	239.1	3.3	4.732	4.732	0.192	−36.0	11

TABLE 2—*Continued*

HIP[a]	Name[b]	R.A.[c]	Decl.[c]	T_{int} [d]	T_{lin} [d]	σ_T [e]	D_{int} [f]	D_{lin} [f]	σ_D [g]	V_r [h]	Reference[i]
42049	HD 72617	08 34 13.35	+08 27 08.5	−1063.9	−1064.2	150.8	4.762	4.748	0.818	53.0	12
52097	HD 92184	10 38 43.16	+05 44 02.4	6984.0	7349.4	961.8	4.770	2.803	4.182	−9.2	CfA
106440......	Gl 832	21 33 34.02	−49 00 25.3	−51.5	−51.5	34.4	4.828	4.828	0.158	4.1	15
82003	Gl 638	16 45 06.38	+33 30 29.9	230.1	230.1	1.0	4.834	4.834	0.074	−31.4	CfA
89937	Gl 713	18 21 02.34	+72 44 01.3	−155.5	−155.5	0.2	4.838	4.838	0.032	32.4	34
110294......	HD 239927	22 20 25.74	+58 05 05.3	1569.8	1570.6	173.6	4.871	4.890	1.042	−35.5	15
80459	Gl 625	16 25 24.19	+54 18 16.3	220.6	220.7	0.9	4.896	4.896	0.070	−13.0	CfA
39780	HD 67228	08 07 45.84	+21 34 55.1	598.8	598.8	17.2	4.924	4.925	0.247	−36.4	35
92871	Gl 735	18 55 27.36	+08 24 09.6	688.0	687.9	98.1	4.927	4.927	0.924	−13.5	11
43670	HD 75935	08 53 49.93	+26 54 47.7	2063.5	2065.2	109.3	4.938	5.063	1.101	−18.9	36
53985	Gl 410	11 02 38.25	+21 58 02.2	529.6	529.7	16.3	4.976	4.980	0.238	−17.6	37
27693	HD 39655	05 51 47.13	−44 00 52.0	−3403.0	−3421.0	389.1	4.979	5.197	1.555	29.3	38
82817	Gl 644	16 55 29.24	−08 20 03.1	−73.6	−73.6	2.5	4.982	4.982	0.159	18.8	17
67529	HD 120702	13 50 08.10	+42 33 26.2	2120.5	2132.7	177.9	4.993	5.184	0.963	−44.0	39

[a] *Hipparcos* Catalogue number.
[b] Alternative identification.
[c] Right ascension and declination for epoch J1991.25, as given in the *Hipparcos* Catalogue. Units of right ascension are hours, minutes, and seconds, and units of declination are degrees, arcminutes, and arcseconds.
[d] Time of closest approach (10^3 yr) for integrated orbits (T_{int}) and for rectilinear motion (T_{lin}). The sign indicates a past (negative sign) or future (positive sign) passage.
[e] Time uncertainty (10^3 yr).
[f] Closest approach distance (pc) for integrated orbits (D_{int}) and for rectilinear motion (D_{lin}).
[g] Distance uncertainty (pc).
[h] Radial velocity (km s^{-1}).
[i] Radial velocity reference: CfA denotes measurements by the Center for Astrophysics; (1) Matthews & Gilmore 1993; (2) Wesselink 1953; (3) Wilson 1953; (4) Holberg, Bruhweiler, & Andersen 1995; (5) Marcy, Lindsay, & Wilson 1987; (6) Nordström & Andersen 1985; (7) Beavers & Eitter 1986; (8) Rodgers & Eggen 1974; (9) Fehrenbach & Duflot 1982; (10) Abt, Sanwal, & Levy 1980; (11) Gliese & Jahreiss 1991; (12) Fehrenbach et al. 1997; (13) Duquennoy & Mayor 1991; (14) Andersen & Nordström 1983; (15) Barbier-Brossat 1989; (16) Smak & Preston 1965; (17) Evans 1978; (18) Feast 1970; (19) Wilson 1967; (20) Beavers et al. 1979; (21) Greenstein & Trimble 1967; (22) Batten & Fletcher 1971; (23) Duflot et al. 1995; (24) Jones & Fisher 1984; (25) Bopp & Meredith 1986; (26) Barnes, Moffett, & Slovak 1986; (27) Ginestet et al. 1985; (28) Tomkin & Pettersen 1986; (29) Abt 1970; (30) Soderblom & Mayor 1993; (31) Catchpole et al. 1982; (32) Evans 1959; (33) Fehrenbach et al. 1987; (34) Tomkin et al. 1987; (35) Abt & Levy 1976; (36) Orosz, Wade, & Harlow 1997; (37) Young, Sadjadi, & Harlan 1987; (38) Evans, Mezies, & Stoy 1957; (39) Duflot et al. 1990.

within a few Myr. Some passages have a large uncertainty, mainly because of large errors in the measured parallax or proper motion; the miss distances and encounter times reported for these passages should be considered with caution.

We find good agreement between the values for the linear approximation and the values for the integrated Galactic orbits for most of the stars in Table 2. This is basically due to the relatively short encounter times for most of the trajectories of these nearby stars. As larger times are considered the disagreement grows, as would be expected (see § 2). The major fraction of the stars with larger disagreements also have large values of the error estimate δ_{total} discussed above.

The closest approach distances versus time of past (negative times) or future (positive times) encounters are shown in Figure 1. Stars coming within about 2–3 pc may be potential perturbers of the Oort cloud. The size of the data point for each star is proportional to the visual brightness of the star at the predicted minimum distance. From this plot we see that the passages at large times are dominated by stars with the largest apparent brightnesses at closest approach. This suggests an observational bias, which can be explained if one notes that most of the stars that had or will have a close passage at large times from the present epoch could only have been observed by *Hipparcos* if they are intrinsically bright.

This bias is also seen if one considers the frequency of stellar approaches versus time, as shown in Figure 2. The distribution is sharply peaked towards the current epoch and falls off rapidly within ± 1 Myr of the present time.

The frequency of stellar passages within any distance, D, of the Sun can be estimated by $N = \pi D^2 v_\odot \rho_*$, where $v_\odot$ is the velocity of the Sun relative to the stars and ρ_* is the local density of stellar systems. Mignard (1998) found values for the solar motion of 16.1–21.2 km s^{-1} relative to the local standard of rest as measured relative to various stellar types, based on *Hipparcos* data for stars within 2 kpc of the Sun and within 30° of the Galactic plane. Also using *Hipparcos* data, Mignard found that the velocity dispersions of stars in the solar neighborhood ranged between 17.1 and 42.6 km s^{-1}, again depending on stellar type. We assume a value of 40 km s^{-1}, since most encounters will be with the more numerous, higher velocity, solar-type and late-type stars. If we add this value in quadrature with a nominal value of 20 km s^{-1} for the solar motion, then the mean encounter velocity of stars or star systems with the Sun, $v_\odot$, is on the order of 45 km s^{-1}.

A current best estimate for the local density of stellar systems (single or multiple stars), ρ_*, within 5 pc of the Sun is 0.086 pc^{-3} (T. J. Henry 1998, private communication). Combining this value with the nominal value of 45 km s^{-1} for $v_\odot$ found above and assuming an encounter distance of ≤ 1 pc, gives $N = 12.4$ Myr^{-1}. Earlier estimates by Weissman (1980) and Fernandez & Ip (1991) found values for N of 5.1 and 7 Myr^{-1}, respectively, assuming somewhat different input values (i.e., in general, lower encounter velocities).

A logarithmic plot of the cumulative number of predicted stellar encounters from our *Hipparcos* data, between the Sun and passing stars within 5 pc, is shown in Figure 3. These data are for 86 stellar systems in our sample with measured radial velocities and encounter times within ± 1 Myr. The dashed line in the figure is a least-squares fit to the data, which has a slope of 2.12 ± 0.04, in fair agreement with theory. Assuming similar statistics for the total sample,

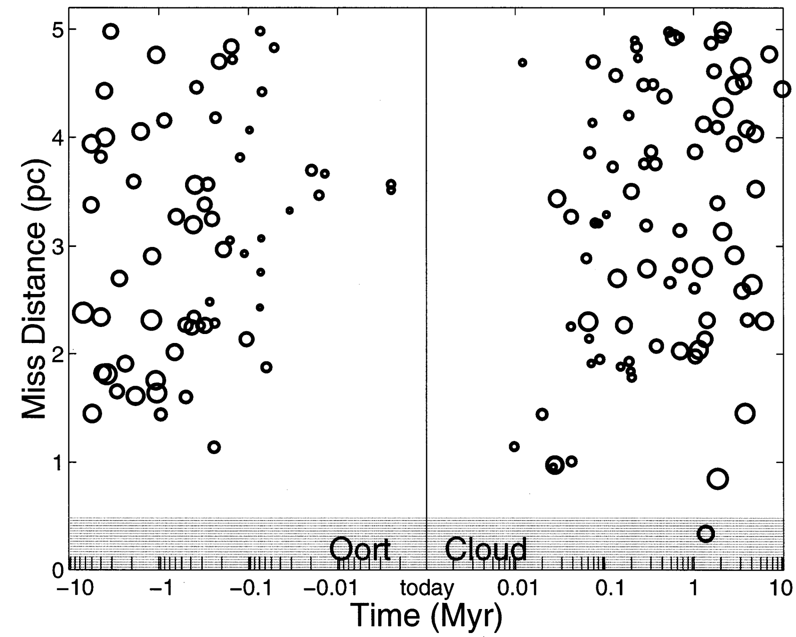

FIG. 1.—Miss distance (pc) vs. time (Myr) of predicted stellar approaches within 5 pc. The outer radius of the Oort cloud is approximately 10^5 AU. The size of each dot is proportional to the star's visual brightness at closest approach (stars with bigger circles are brighter). These visual magnitudes range between −3.5 and 12.

we find a value of 3.5 stellar systems per Myr passing within 1 pc, considerably less than the value estimated above. For the stars in our sample, the rms encounter velocity with the solar system is 52 km s^{-1}, in good agreement with the estimate above.

The apparent disagreement in the encounter rates is likely due to observational incompleteness in our sample. The *Hipparcos* Catalogue is complete to a visual magnitude of ∼(7.3–9.0), depending on Galactic latitude and spectral type and has a limiting visual magnitude of ∼12. Consequently, fainter, low-mass stars near the periphery of our search area were likely missed. This observational incompleteness is also evident in the decrease in encounter frequency and the increase in the mean brightness of the stars encountering the solar system as one moves away from the present epoch in time, as shown in Figures 1 and 2.

The incompleteness in the *Hipparcos* Catalogue is evident if one considers the statistics of stars in the solar neighborhood. T. J. Henry (1998, private communication) found a local density of 0.086 star systems pc^{-3} within 5 pc of the Sun. This compares with 0.067 star systems pc^{-3} for the

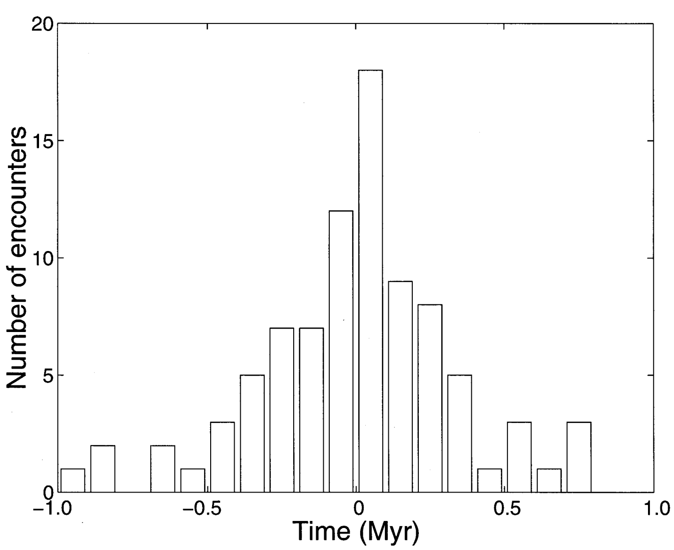

FIG. 2.—Number of encounters within 5 pc as a function of time (Myr) for the encounters within ±1 Myr.

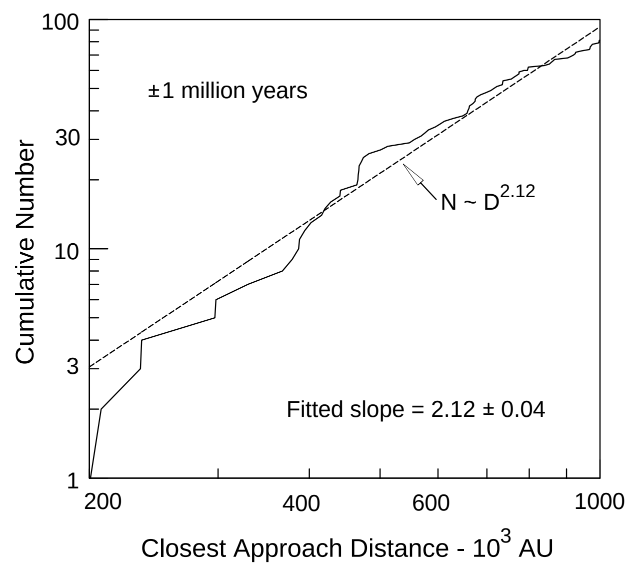

FIG. 3.—Logarithmic plot of the cumulative number of predicted stellar encounters vs. closest approach distance (10^3 AU) within ±1 Myr. The dashed line is a least-squares fit to the data. The slope of 2.12 ± 0.04 is in fair agreement with theoretical expectations. The predicted encounter rate is 3.5 stars Myr^{-1} pc^{-2}, less than predicted values. This is likely because of observational incompleteness in the *Hipparcos* data set.

Hipparcos Catalogue within 5 pc. Henry also found a density of 0.055 pc^{-3} within 10 pc of the Sun, which he noted was substantially incomplete (see also Henry et al. 1997); the corresponding density for the *Hipparcos* Catalogue is 0.041 pc^{-3} within 10 pc. For the star systems in our sample that will encounter the solar system within 5 pc, the rms current distance is 13.9 pc, so we would expect that the incompleteness in our estimate to substantially exceed 50%.

If we only consider stellar encounters with the solar system within ± 0.5 Myr, we find $N = 6.4D^{2.09 \pm 0.03}$. This is almost double the estimate for the ± 1 Myr interval, but still only about one-half of that estimated by the theoretical calculation above. We suggest that this is further proof that observational incompleteness exists within our sample and is a strong function of encounter time and current stellar distance. We will examine the question of observational incompleteness in more detail in a future paper.

3.1. *Past and Future Close Approaches*

From Table 2 we see that 147 stars are predicted to come within a distance of 5 pc during a time interval of about ± 10 Myr, with roughly similar numbers of close approaches in the past and the future: 64 and 83, respectively. For all stars with a closest approach distance of less than 3 pc, the variation with time of the separation distance between each star and the Sun is shown in Figures 4 and 5 for time intervals of 2 Myr in the past and 2 Myr in the future, respectively.

The star with the closest future passage in the sample is Gl 710. The predicted minimum distance for this star is 0.336 pc (69×10^3 AU) with the integrated orbit and 0.343 pc (71×10^3 AU) with the linear motion model; the encounter time is 1.36 Myr in the future (see discussion below for the assumptions made in these calculations). This star is the only one in our sample with a predicted miss distance less than 10^5 AU (~ 0.5 pc).

Close stellar passages within 3 pc of the Sun during a time span of $\pm 10^5$ yr from the present are shown in Figure 6. The best-determined miss distances for our sample are obtained for this interval of time. The trajectories of the stars are plotted along with the corresponding uncertainties in the distance and time of closest approach. Several stars come within ~ 1 pc of the Sun.

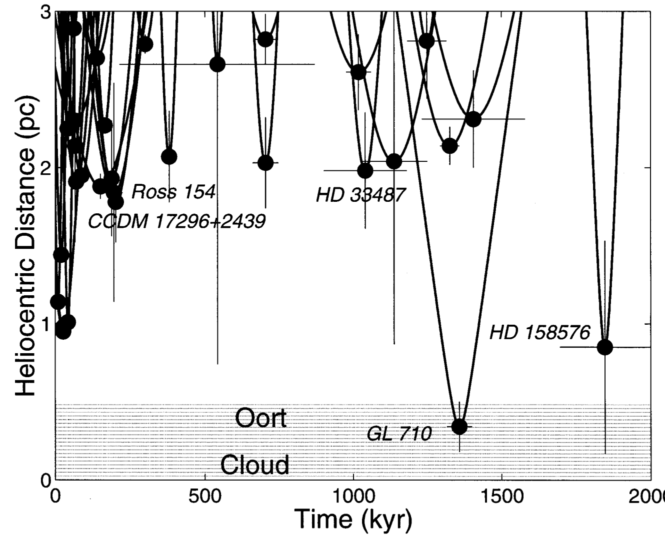

FIG. 5.—Same as Fig. 4, but up to 2 Myr in the future. Gl 710 has the most plausible passage through the Oort cloud in our sample. Stars having predicted close passages within the next 0.1 Myr are identified in Fig. 6.

Proxima Centauri (HIP 70890) is currently the nearest star to the Sun. Based on its proximity on the plane of the sky and similar distance, Proxima is commonly thought to be a third component of the binary system α Centauri A/B (HIP 71683 and 71681). However, kinematic data do not allow a bound orbit for Proxima to be unambiguously determined. The value of -15.7 ± 3.3 km s^{-1} for the radial velocity of Proxima (Thackeray 1967) raises some questions about the bound hypothesis (see Matthews & Gilmore 1993 and Anosova, Orlov, & Pavlova 1994 for discussion). On the other hand, a value of -21.7 ± 1.8 km s^{-1} based on more precise unpublished measurements of the radial velocity of Proxima made during ESO's Coravel

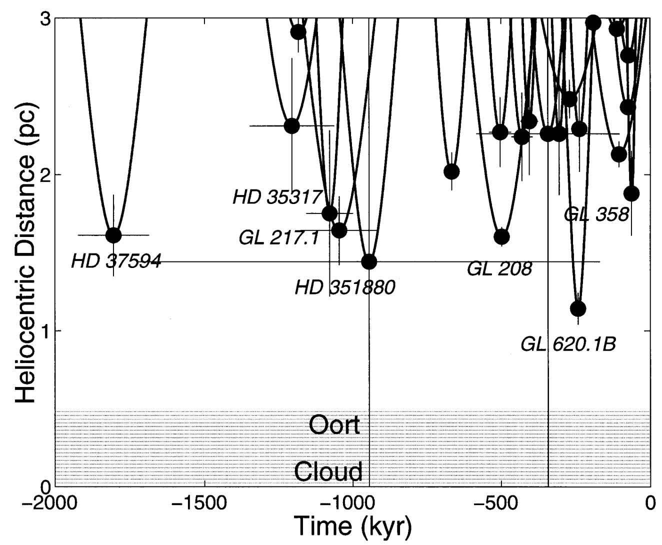

FIG. 4.—Closest predicted stellar passages within the past 2 Myr. Error bars in time and miss distance are plotted at the closest approach point.

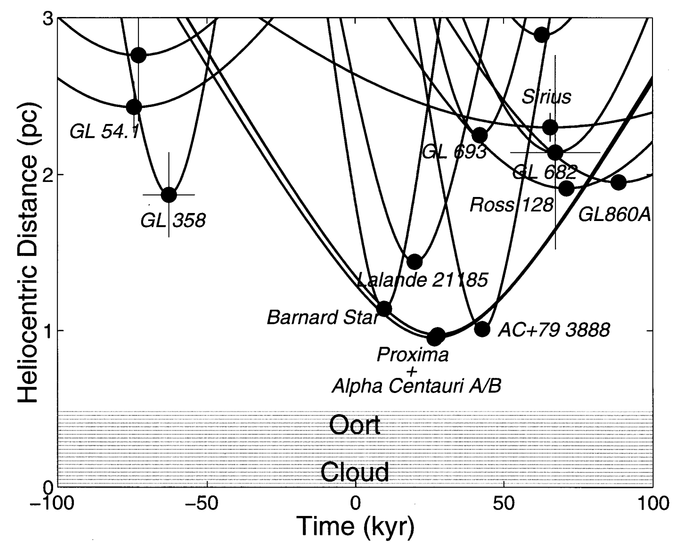

FIG. 6.—Same as Figs. 4 and 5, but for $\pm 10^5$ yr. Several close passages are predicted over the next few tens of thousand years.

program, led Matthews & Gilmore (1993) to suggest that Proxima is a bound member of the α Centauri system. Matthews (1994) used a radial velocity of -22.37 km s^{-1} for Proxima, required to account for the bound hypothesis with the implied semimajor axis of Proxima's orbit. Matthews found a closest approach distance to the Sun for Proxima of 0.941 pc, which is 26.7×10^3 yr from now. For the α Centauri A/B system he found a closest approach distance of 0.957 pc in about 28.0×10^3 yr. Our results of 0.954 pc in 26.7×10^3 yr for Proxima (using the radial velocity value of -21.7 km s^{-1}) and 0.974 pc in 27.8×10^3 yr for the barycenter of α Centauri A/B are consistent with these earlier predictions. Also in good agreement is the close passage of Barnard's star (HIP 87937), which will have its closest approach to the Sun 9.7×10^3 yr from now at a distance of 1.143 pc according to our results.

In the study carried out by Mülläri & Orlov (1996), several close encounters with the Sun are predicted using data from the Preliminary Version of the Third Catalogue of Nearby Stars (Gliese & Jahreiss 1991). For their calculations they considered both straight-line motion of the stars with respect to the Sun and also the motion of the stars in the Galactic potential model of Kutuzov & Ossipkov (1989). They find good agreement between the results from both methods.

In general, the values of Mülläri & Orlov for the stars contained in our sample are in agreement with our results, though there are some differences as well. In particular, Gl 473, which was not observed by *Hipparcos* because it is too faint (visual magnitude 12.5; Landolt 1992), is predicted by Mülläri & Orlov to have a future closest approach of 60×10^3 AU in 7500 yr. However, the radial velocity of -553.7 km s^{-1} listed in the catalogue for this star is much too high, so the predicted miss distance should actually be much larger. Gl 473, a very low mass binary system (see, e.g., Schultz et al. 1998), is reported to have radial velocities of -5.0 km s^{-1} (Wilson 1953), $+19.0$ km s^{-1} (Reid, Tinney, & Mould 1994), and $+6.7$ km s^{-1} (Reid, Hawley, & Gizis 1995). Based on 29 exposures measured with the CfA digital speedometers covering more than 2500 days, we find a system radial velocity of $+5.6 \pm 0.7$ km s^{-1} for the binary system Gl 473. Using this radial velocity we find a closest approach distance of 878×10^3 AU, 17,000 yr in the past.

For Gl 710, Mülläri & Orlov predict a future close approach distance of 259×10^3 AU in about 1 Myr assuming linear motion, and 279×10^3 AU in about 1 Myr using the Galactic potential model, compared with our values of 71×10^3 AU and 69×10^3 AU, respectively, in about 1.36 Myr. The difference between their results and ours for Gl 710 is mainly due to the much larger (about 5 times larger) ground-based proper-motion value reported for this star in the Catalogue of Nearby Stars, than the one measured by *Hipparcos*.

3.2. *The Future Close Passage of Gl 710*

Gl 710 is a late-type dwarf star (dM1 according to Joy & Abt 1974; K7 V according to Upgren et al. 1972), currently located at a distance of 19.3 pc from the Sun, with an estimated mass of 0.4–0.6 $M_\odot$ and a visual magnitude of 9.66. Based on its very small proper motion and using a radial velocity of -23 km s^{-1}, Vyssotsky (1946; see also Gliese 1981 and Gliese, Jahreiss, & Upgren 1986) predicted that Gl 710 will have a close passage with a minimum distance of less than 1 pc in about 0.5 Myr. However, in the Preliminary Version of the Third Catalogue of Nearby Stars, Gliese & Jahreiss (1991) list a considerably smaller radial velocity for Gl 710, -13.3 km s^{-1}, based on the value reported by Stauffer & Hartmann (1986). Because this change in the radial velocity has such a large impact on the time and distance calculated for the closest approach, we have looked carefully at the published data and have made new velocity measurements of our own.

There is some evidence that Gl 710 may be a binary, but that evidence is far from conclusive. Astrometric residuals in earlier proper-motion measurements suggested a possible periodicity of 1700 days (Osvalds 1957). A slight indication of a period of this order was also found by Grossenbacher, Mesrobian, & Upgren (1968), although they did not consider it to be of great significance. However, a speckle measurement of this star did not detect any companion with $\Delta m \leq 3$ and angular separation in the range 0″.05–1″ (Blazit, Bonneau, & Foy 1987). Furthermore, the *Hipparcos* astrometric data do not show any evidence of a nonlinear proper motion during an observation period of 3.4 yr.

There is some spectroscopic evidence that the radial velocity of Gl 710 may have changed by about 10 km s^{-1} over the past 50 yr. We list in Table 3 the radial velocities reported in the literature plus five new values measured with the CfA digital speedometers. The first four values in Table 3 (Abt 1973) are from observations at the Mount Wilson Observatory, and their weighted mean, -23.3 km s^{-1}, quality b, is reported in the General Catalogue of Stellar Radial Velocities (Wilson 1953).

Based on the values listed in Table 3, Gl 710 appears to exhibit a long-term radial velocity drift of about 10 km s^{-1} over 50 yr. The measurements made in the 1940s show radial velocities more negative than -20 km s^{-1}, whereas the observations between 1984 and 1998 report values less negative than -15 km s^{-1} (with the sole exception of the value of -26.3 ± 15.0 km s^{-1}, which can be discounted due to its large uncertainty).

However, we believe that this radial-velocity difference may not be real and may instead be due to a systematic error in the zero point of the four Mount Wilson observations made in the 1940s. As far as we can tell, all of the older velocities are derived from the same four Mount Wilson spectra (Abt 1973; Joy & Mitchell 1948; Vyssotsky

TABLE 3

RADIAL VELOCITY MEASUREMENTS FOR GL 710

Date[a]	V_r[b]	Reference
1944 Sep 7	-21.5	Abt 1973
1944 Sep 23	-20.2	Abt 1973
1945 Aug 29	-23.0	Abt 1973
1945 Sep 29	-26.6	Abt 1973
Not reported......	-22.8 ± 0.9	Vyssotsky 1946
Not reported......	-23	Joy & Mitchell 1948
1984 Mar 4	-14.3	Stauffer & Hartmann 1986
1993 Sep 8	-26.3 ± 15.0	Reid et al. 1995
1994 May 23......	-13.5 ± 2.0	Gizis 1997
1996 Oct 5	-13.89 ± 0.28	CfA
1996 Oct 6	-13.75 ± 0.30	CfA
1996 Oct 8	-13.73 ± 0.40	CfA
1997 May 17......	-14.05 ± 0.37	CfA
1998 Mar 15	-14.08 ± 0.57	CfA

[a] Date of observation.

[b] Radial velocity (km s^{-1}).

1946). To assess the zero point of the old Mount Wilson velocities, we have compared the radial velocities of 27 single stars (including Gl 710) observed at Mount Wilson and listed by Joy & Mitchell (1948) with measurements of the same stars made at CfA. We find a mean difference (CfA − Mount Wilson) of about 9 km s^{-1} and an rms difference of 7.4 km s^{-1}.

Furthermore, there is no evidence for any drift in the recent CfA velocities. Although these observations span only 520 days, the allowed velocity drift is only a few tenths of a km s^{-1} at most.

In addition, it can be argued that it would be unlikely for an unseen main-sequence companion to produce the suggested drift of about 10 km s^{-1} over 50 yr. Such a companion could not be more massive than about 0.3 or 0.4 $M_{\odot}$, otherwise its spectrum would have been seen and it would have been detected by the speckle observations. However, a circular orbit for such a companion with a period of 100 yr would produce a velocity amplitude of at most about ± 6 km s^{-1}. One way to get a larger velocity amplitude would be to invoke an unseen evolved remnant for the companion, such as a massive (but cool) white dwarf. But then the astrometric motion of Gl 710 would have to be large, on the order of 1″ amplitude for the full orbit. For an orbital period of 100 yr, the motion during the *Hipparcos* mission would hardly have departed from a straight-line segment, but it would have been absorbed in the proper-motion measurement. This would require that the orbital motion of Gl 710 just happened to cancel out the space motion of the system at the time of the *Hipparcos* mission. However, the proper motion was also measured to be very small by Vyssotsky (1946), and therefore the orbital and space motion would also have cancelled 50 yr ago. This is not consistent with supposing that the system was in a significantly different phase of its orbit, as would be required to explain the radial-velocity difference. Another way to increase the velocity amplitude would be to invoke a shorter period orbit, but this too would also be difficult to reconcile with the observations.

Therefore, we conclude that Gl 710 is not a binary, and we have adopted the mean of the recent CfA values, -13.9 ± 0.2 km s^{-1}, for its radial velocity. We caution that the possible binary nature of Gl 710 has not been completely ruled out, and additional monitoring of the radial velocity and/or astrometric positions over the coming years or even decades is clearly desirable for settling this issue. Adopting a mean radial velocity of -13.9 km s^{-1} from the five recent CfA measurements, we obtain the miss distance and encounter time listed in Table 2.

The *Hipparcos* proper-motion measurement for Gl 710 could be improved by *VLBI* astrometric observations if the star were a sufficiently strong radio emitter (at least 1 mJy). Since Gl 710 has been designated as a late-type dwarf star it might be a detectable radio source. We observed Gl 710 at 8.4 GHz with the VLA[2] on 1997 January 21 to determine its flux density as a precursor to possible *VLBI* observations. No radio emission was detected from Gl 710 with a conservative upper limit of 0.2 mJy.

[2] The National Radio Astronomy Observatory is a facility of the National Science Foundation operated under cooperative agreement by Associated Universities, Inc.

4. DYNAMICAL EFFECT ON THE OORT CLOUD

The dynamical effect of a stellar passage on the Oort cloud depends not only on its proximity but also on the mass of the star and how long each encounter lasts. The relative influence of the stars on the cometary orbits can be estimated from the differential attraction exerted on the Sun and on a comet in the cloud, which results in a net change in the velocity of the comet relative to the Sun. The velocity impulse, ΔV, on an Oort cloud comet or on the Sun as a result of a single stellar passage is approximately equal to $2GM_* V_*^{-1} D^{-1}$, where G is the gravitational constant, M_* is the mass of the star, V_* is its total velocity relative to the Sun, and D the miss distance (Oort 1950). The velocity impulse is directed at the star's point of closest approach. The relative magnitude of the differential velocity perturbation between the comet and the Sun can be estimated by multiplying ΔV by a term r/D, where r is the distance between the comet and the Sun.

In addition, the cumulative effect of close passages of several stars not necessarily belonging to the same multiple system but closely spaced in time may also play a role. Stochastic encounters with stars sufficiently massive and closely spaced in time should result in a somewhat larger effect than considering them separately. However, to be significant, such encounters would need to be spaced at intervals less than or equal to the time for a typical star to transit the Oort cloud. For instance, if we take a star's path length of 10^5 AU through the outer Oort cloud (miss distance of about 86×10^3 AU), and a typical stellar encounter velocity of 45 km s^{-1}, then the star passages would need to be spaced within $\sim$11,000 yr to have a cumulative effect. Several temporal groups of encounters are present in our data. However, the uncertainties in the close approach times are typically larger than the Oort cloud transit time estimated above, and thus we cannot reliably say that any of these groups are real. In addition, since the effects of these random encounters will add stochastically, we see no evidence for temporal groups whose cumulative effect would be more significant than the individual closest single-star passages that we have identified.

The relative magnitudes of the strongest predicted stellar perturbations on the Oort cloud, as derived from the above considerations, are listed in Table 4 and shown in Figure 7 for the greatest potential perturbers. The magnitudes are given in arbitrary units and represent a first-order measure of the gravitational influence of one close stellar passage relative to the others. This identifies the stars most likely to perturb the Oort cloud. However, the actual perturbation on the cometary orbits can only be estimated through dynamical simulations.

The most significant perturber in our data set is, as expected, Gl 710 (HIP 89825). A mass of 0.6 $M_{\odot}$ has been used for Gl 710. The second largest potential perturber is Algol (HIP 14576), a triple-star system with a total mass of 5.8 $M_{\odot}$ (Martin & Mignard 1998). The close encounter of Algol was determined by Lestrade et al. (1998) to be 3 pc, 7.3 Myr ago, using *VLBI* astrometry. These values are in agreement, within the uncertainties, with our values of 2.7 pc (linear motion model) and 2.4 pc (integrated orbit) 6.9 Myr ago. Algol's large total mass and low encounter velocity compensate for the comparatively larger miss distance.

We conducted dynamical simulations of stars passing close to the Oort cloud, in order to evaluate further the

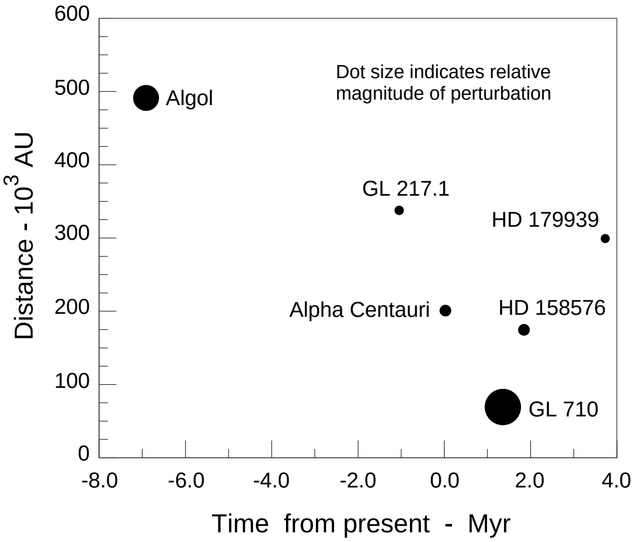

FIG. 7.—Relative magnitude of the largest perturbers on the Oort cloud in our sample. The relative magnitude of the perturbation is proportional to $M_* r/V_* D^2$, where M_* and V_* are the mass and encounter velocity of the star, respectively, r is the radius of the Oort cloud, and D is the miss distance. Dot size indicates the relative magnitude of the perturbation.

possible perturbative effects of our predicted closest stellar encounters. We used the dynamical model of Weissman (1996b), which uses the impulse approximation to estimate the velocity impulses on the Sun and on hypothetical comets, and thus the changes in the orbits of comets in a modeled Oort cloud. The simulations confirmed the relative expected magnitude of the perturbations shown in Table 4.

Based on simulations containing 10^8 hypothetical comets, we find that the maximum effect occurs, as expected, for the encounters with Gl 710. This star results in a minor shower with $\sim 4 \times 10^{-7}$ of the Oort cloud population being thrown into Earth-crossing orbits. Assuming an estimated Oort cloud population of 6×10^{12} comets (Weissman 1996a), this predicts a total excess flux of about 2.4×10^6 Earth-crossing comets in each shower.

However, because the arrival times of the comets are spread over about 2×10^6 yr, the net increase in the Earth-crossing cometary flux is only about one new comet per year. This can be compared with the estimated steady-state flux of ~ 2 dynamically new (i.e., comets entering the planetary system directly from the Oort cloud) long-period comets per year (Weissman 1996a). Thus, the net increase in the cometary flux is about 50%. Since long-period comets likely account for only about 10% of the steady-state impactor flux at Earth (Weissman 1997), the net increase in the cratering rate is about 5%. This small increase is likely not detectable given the stochastic nature of comet and asteroid impacts.

5. CONCLUSIONS

The study of the possible perturbation of the Oort cloud by passing stars has important implications for our understanding of the solar system. The identification of potential perturbers is thus necessary not only to estimate the recent past cometary flux caused by close stellar encounters and its possible correlation with the observed impact rate on Earth, but also to predict future passages and to estimate their perturbative effect.

In this paper we have studied the close passages of stars using *Hipparcos* data. Radial velocity measurements from the literature plus others from our own observations have been used to estimate the heliocentric velocities of these stars and to calculate their passages. We have used both a rectilinear motion model and the integrated orbits in the Galactic potential. The good agreement between the two models for most of the stars passing within a few million years supports the criteria used to select the sample. From our data set we derive a rate of close stellar passages of $3.5D^{2.12}$ stellar systems per Myr, where D is the miss distance considered. We consider this value a lower limit since there is considerable evidence for observational incompleteness in our sample.

We have identified several stars whose close passage could cause a significant perturbation of the Oort cloud. In order to investigate the effect of such passages on the cometary orbits, we have carried out dynamical simulations. This is the first time that such simulations have been performed for actual stellar passages. In general, the effect of these passages depends not only on the miss distance but also on the total mass of the star system and on its relative

TABLE 4

POTENTIAL PERTURBERS OF THE OORT CLOUD

Name	HIP	T[a]	D[b]	M[c]	V[d]	Relative Magnitude[e]
Gl 710	89825	1357.8	0.336	0.6	14	100
Algol	14576	−6916.0	2.381	5.8	4	66
HD 158576.............	85661	−1846.5	0.846	2.3	46	18
Proxima + α Cen......	71681[f]	27.7	0.974	2.13	33	18
Gl 217.1	27288	−1045.9	1.637	2.0	20	10
HD 179939.............	94512	3734.0	1.451	2.2	31	9

[a] Time of closest passage ($\times 10^3$ yr).
[b] Miss distance (in pc).
[c] Mass (in $M_\odot$). Values for Gl 710, HD 158576, and HD 179939 are estimated. Value for Algol from Martin & Mignard 1998. Value for Proxima + α Cent from Kamper & Wesselink 1978. Value for Gl 217.1 from Malagnini & Morossi 1990.
[d] Space velocity (in km s^{-1}).
[e] Relative magnitude of the potential perturbation in arbitrary units. The values are proportional to $M_* r V_*^{-1} D^{-2}$ and are normalized to have value 100 for the largest potential perturbation.
[f] The HIP number given is for the α Centauri B component, but the total mass is for the triple system Proxima Centauri and α Centauri A/B.

velocity. Therefore, a suitable combination of mass and velocity might result in a larger perturbation for more distant passages than for closer ones.

We find little evidence for any close stellar encounters in the recent past. This lack of recent close stellar passages is in agreement with analyses by Weissman (1993) and Fernandez (1994), who found no evidence for a recent major perturbation of the Oort cloud.

For the future passage of Gl 710, the star with the closest approach in our sample, we predict that about 2.4×10^6 new comets will be thrown into Earth-crossing orbits, arriving over a period of about 2×10^6 yr. Many of these comets will return repeatedly to the planetary system, though about one-half will be ejected on the first passage. These comets represent an approximately 50% increase in the flux of long-period comets crossing Earth's orbit.

From our estimated miss distances we conclude that no substantial enhancement of the steady-state cometary flux would result (or would have resulted) from the stars in our sample. However, further measurements of radial, as well as transverse, velocities are required to improve the accuracy of the estimates of the close approach distances for stars that are possible members of binary or multiple systems. Further measurements are also required for stars for which the possibility of a very close or even penetrating passage through the Oort cloud still remains open, because of the large errors in their predicted miss distances.

We thank J. E. Gizis, T. J. Henry, H. Jahreiss, J. Kovalevsky, and J. R. Stauffer for kindly providing us with information on several stars; E. García-Górriz for her support on MATLAB programming; and R. Asiaín, J. M. Paredes, and J. Núñez for helpful discussions. We also thank an anonymous referee for his/her suggestions to improve the paper. This research is based on data from the *Hipparcos* astrometry satellite and has also made use of the Simbad database, operated at CDS, Strasbourg, France. This research was carried out in part at the Jet Propulsion Laboratory, California Institute of Technology, under contract with the National Aeronautics and Space Administration

REFERENCES

Abt, H. A. 1970, ApJS, 19, 387
———. 1973, ApJS, 26, 365
Abt, H. A., & Levy, S. G. 1976, ApJS, 30, 273
Abt, H. A., Sanwal, N. B., & Levy, S. G. 1980, ApJS, 43, 549
Andersen, J., & Nordström, B. 1983, A&A, 122, 23
Anosova, J., Orlov, V. V., & Pavlova, N. A. 1994, A&A, 292, 115
Antonov, V. A., & Latyshev, I. N. 1972, in The Motion, Evolution of Orbits and Origin of Comets, ed. G. A. Chebotarev, E. I. Kazimirchak-Polonskaya, & B. G. Marsden (Dordrecht: Reidel), 341
Barbier-Brossat, M. 1989, A&AS, 80, 67
Barnes, T. G., III, Moffett, T. J., & Slovak, M. H. 1986, PASP, 98, 223
Batten, A. H., & Fletcher, J. M. 1971, PASP, 83, 149
Beavers, W. I., & Eitter, J. J. 1986, ApJS, 62, 147
Beavers, W. I., Eitter, J. J., Ketelsen, D. A., & Oesper, D. A. 1979, PASP, 91, 698
Biermann, L., Huebner, W. F., & Lüst, R. 1983, Proc. Natl. Acad. Sci., 80, 5151
Blazit, A., Bonneau, D., & Foy, R. 1987, A&AS, 71, 57
Bopp, B. W., & Meredith, R. 1986, PASP, 98, 772
Catchpole, R. M., Evans, D. S., Jones, D. H. P., King, D. L., & Wallis, R. E. 1982, R. Obs. Bull. Greenwich, No. 188, 5
Crézé, M., Chereul, E., Bienaymé, O., & Pichon, C. 1998, A&A, 329, 920
Dommanget, J., & Nys, O. 1994, Commun. Obs. R. Belgique, 115, 1
Duflot, M., Fehrenbach, C., Mannone, C., Burnage, R., & Genty, V. 1995, A&AS, 110, 177
Duflot, M., Fehrenbach, C., Mannone, C., & Genty, V. 1990, A&AS, 83, 251
Duquennoy, A., & Mayor, M. 1991, A&AS, 248, 485
ESA. 1997, The Hipparcos and Tycho Catalogues (ESA SP-1200) (Noordwijk: ESA)
Evans, D. S. 1959, MNRAS, 119, 526
———. 1978, Bull. Inf. CDS, No. 15, 121
Evans, D. S., Menzies, A., & Stoy, R. H. 1957, MNRAS, 117, 534
Farley, K. A., Montanari, A., Shoemaker, E. M., & Shoemaker, C. S. 1998, Science, 280, 1250
Feast, M. W. 1970, MNRAS, 148, 489
Feast, M. W., & Whitelock, P. 1997, MNRAS, 291, 683
Fehrenbach, C., & Duflot, M. 1982, A&AS, 48, 409
Fehrenbach, C., Duflot, M., Burnage, R., Mannone, C., Peton, A., & Genty, V. 1987, A&AS, 71, 275
Fehrenbach, C., Duflot, M., Mannone, C., Burnage, R., & Genty, V. 1997, A&AS, 124, 255
Fernandez, J. A. 1994, in IAU Symp. 160, Asteroids, Comets, Meteors, ed. A. Milani, M. Di Martino, & A. Cellino (Dordrecht: Kluwer), 223
Fernandez, J. A., & Ip, W.-H. 1987, Icarus, 71, 46
Fernandez, J. A., & Ip, W.-H. 1991, in Comets in the Post-Halley Era, ed. R. L. Newburn, M. Neugebauer, & J. Rahe (Dordrecht: Kluwer), 487
Gieren, W. P. 1989, A&A, 225, 381
Ginestet, N., Carquillat, J. M., Pédoussant, A., & Nadal, R. 1985, A&A, 144, 403
Gliese, W. 1981, Sterne Weltraum, 20, 445
Gliese, W., & Jahreiss, H. 1991, Preliminary Version of the Third Catalogue of Nearby Stars, unpublished
Gliese, W., Jahreiss, H., & Upgren, A. R. 1986, in The Galaxy and the Solar System, ed. R. Smoluchowski, J. N. Bahcall, & M. S. Matthews (Tucson: Univ. Arizona Press), 13
Greenstein, J. L., & Trimble, V. L. 1967, ApJ, 149, 283
Grossenbacher, R., Mesrobian, W. S., & Upgren, A. R. 1968, AJ, 73, 744
Henry, T. J., Ianna, P. A., Kirkpatrick, J. D., & Jahreiss, H. 1997, AJ, 114, 388
Hillenbrand, L. A., Strom, S. E., Vrba, F. J., & Keene, J. 1992, ApJ, 397, 613
Hills, J. G. 1981, AJ, 86, 1730
Holberg, J. B., Bruhweiler, F. C., & Andersen, J. 1995, ApJ, 443, 753
Hut, P., Alvarez, W., Elder, W. P., Hansen, T., Kauffman, E. G., Keller, G., Shoemaker, E. M., & Weissman, P. R. 1987, Nature, 329, 118
Jones, D. H. P., & Fisher, J. L. 1984, A&AS, 56, 449
Joy, A. H., & Abt, H. A. 1974, ApJS, 28, 1
Joy, A. H., & Mitchell, S. A. 1948, ApJ, 108, 234
Kamper, K. W., & Wesselink, A. J. 1978, AJ, 83, 1653
Kerr, F. J., & Lynden-Bell, D. 1986, MNRAS, 221, 1023
Kurtz, M. J., Mink, D. J., Wyatt, W. F., Fabricant, D. G., Torres, G., Kriss, G. A., & Tonry, J. L. 1992, in ASP Conf. Ser. 25, Astronomical Data Analysis Software and Systems I, ed. D. M. Worrall, C. Biemesderfer, & J. V. Barnes (San Francisco: ASP), 432
Kurucz, R. L. 1992a, in IAU Symp. 149, The Stellar Populations of Galaxies, ed. B. Barbuy & A. Renzini (Dordrecht: Kluwer), 225
———. 1992b, Rev. Mexicana Astron. Astrofis., 23, 187
Kutuzov, S. A., & Ossipkov, L. P. 1989, Soviet Astron., 66, 965
Landolt, A. U. 1992, AJ, 104, 340
Latham, D. W. 1985, in IAU Colloq. 88, Stellar Radial Velocities, ed. A. G. D. Philip & D. W. Latham (Schenectady, N.Y.: Davis), 21
———. 1992, in ASP Conf. Ser. 32, Complementary Approaches to Double and Multiple Star Research, ed. H. A. McAlister & W. I. Hartkopf (Chelsea: ASP), 158
Lestrade, J.-F., Jones, D. L., Preston, R. A., Phillips, R. B., Titus, M. A., Rioja, M. J., & Gabuzda, D. C. 1998, in preparation
Malagnini, M. L., & Morossi, C. 1990, A&AS, 85, 1015
Marcy, G. W., Lindsay, V., & Wilson, K. 1987, PASP, 99, 490
Martin, C., & Mignard, F. 1998, A&A, 330, 585
Matthews, R. A. J. 1994, QJRAS, 35, 1 (erratum 35, 243)
Matthews, R., & Gilmore, G. 1993, MNRAS, 261, L5
Martin, C., & Mignard, F. 1998, A&A, 330, 585
Mignard, F. 1998, A&A, submitted
Mülläri, A. A., & Orlov, V. V. 1996, Earth Moon Planets, 72, 19
Nordström, B., & Andersen, J. 1985, A&AS, 61, 53
Nordström, B., Latham, D. W., Morse, J. A., Milone, A. A. E., Kurucz, R. L., Andersen, J., & Stefanik, R. P. 1994, A&A, 287, 338
Oort, J. H. 1950, Bull. Astron. Inst. Netherlands, 11, 91
Orosz, J. A., Wade, R. A., & Harlow, J. B. 1997, AJ, 114, 317
Osvalds, V. 1957, AJ, 62, 274
Reid, I. N., Hawley, S. L., & Gizis, J. E., 1995, AJ, 110, 1838
Reid, N., Tinney, C. G., & Mould, J. 1994, AJ, 108, 1456
Rodgers, A. W., & Eggen, O. J. 1974, PASP, 86, 742
Schultz, A. B., et al. 1998, PASP, 110, 31
Smak, J. I., & Preston, G. W. 1965, ApJ, 142, 943
Smoluchowski, R., & Torbett, M. 1984, Nature, 311, 38
Soderblom, D. R., & Mayor, M. 1993, AJ, 105, 226
Stauffer, J. R., & Hartmann, L. W. 1986, ApJS, 61, 531
Thackeray, A. D. 1967, Observatory, 87, 79
Tomkin, J., McAlister, H. A., Hartkopf, N. I., & Fekel, F. C. 1987, AJ, 93, 1236
Tomkin, J., & Pettersen, B. R. 1986, AJ, 92, 1424

Upgren, A. R., Grossenbacher, R., Penhallow, W. S., MacConnell, D. J., & Frye, R. L. 1972, AJ, 77, 486
Vyssotsky, A. N. 1946, PASP, 58, 166
Weissman, P. R. 1980, Nature, 288, 242
———. 1993, BAAS, 25, 1063
———. 1996a, in ASP Conf. Ser. 107, Completing the Inventory of the Solar System, ed. T. W. Rettig & J. M. Hahn (San Francisco: ASP), 265
———. 1996b, Earth Moon Planets, 72, 25
Weissman, P. R. 1997, in Near-Earth Objects, ed. J. L. Remo (New York: NY Acad. Sci.), 67
Wesselink, A. J. 1953, MNRAS, 113, 505
Wilson, O. C. 1967, AJ, 72, 905
Wilson, R. E. 1953, General Catalogue of Stellar Radial Velocities (Washington: Carnegie Inst. Washington)
Young, A., Sadjadi, S., & Harlan, E. 1987, ApJ, 314, 272